Available at www.sciencedirect.com

ScienceDirect

journal homepage: www.elsevier.com/locate/he

Preparation and catalysis of poly(N-vinyl-2-pyrrolidone) (PVP) stabilized nickel catalyst for hydrolytic dehydrogenation of ammonia borane

*Tetsuo Umegaki, Jun-Min Yan, Xin-Bo Zhang, Hiroshi Shioyama, Nobuhiro Kuriyama, Qiang Xu**

National Institute of Advanced Industrial Science and Technology (AIST), 1-8-31 Midorigaoka, Ikeda, Osaka 563-8577, Japan

ARTICLE INFO

Article history:
Received 6 February 2009
Received in revised form
27 February 2009
Accepted 2 March 2009
Available online 8 April 2009

Keywords:
Nickel catalyst
PVP stabilized
Hydrolysis
Ammonia borane
Hydrogen generation

ABSTRACT

An amorphous nickel catalyst stabilized by poly(N-vinyl-2-pyrrolidone) (PVP) was synthesized by reduction in an aqueous $NaBH_4/NH_3BH_3$ solution. Both the bare nickel catalyst and the PVP stabilized nickel catalyst contain grains with an amorphous structure after the reduction. The PVP stabilized nickel catalyst maintains high activity for hydrolysis of NH_3BH_3 to generate a stoichiometric amount of hydrogen with the cycle number up to 5, while the reaction rate in the presence of the bare nickel catalyst decreases with cycle number. After five cycles, the PVP stabilized nickel catalyst maintains the amorphous structure, while the agglomeration of nickel in the bare nickel catalyst is observed. The results indicate that PVP prevents agglomeration and crystallization of nickel nanoparticles, leading to higher durability than the bare nickel catalyst.

1. Introduction

Hydrogen has attracted much attention as an alternative energy carrier to satisfy the increasing demand for an effective and clean energy supply because of its abundance, high-energy density, and environmental friendliness [1,2]. The use of hydrogen fuel cells in portable electronic devices or vehicles requires lightweight hydrogen storage or on-board hydrogen generation. Although there have been a large number of reports on hydrogen storage materials [2,3] and on on-board reforming of hydrocarbon into hydrogen [4], there are significant challenges related to the storage and the production of hydrogen. For hydrogen storage materials, the gravimetric and volumetric hydrogen capacities must be improved, whereas for on-board reforming, the difficulty in operating the system at high temperature poses an obstacle to its practical application. Boron- and nitrogen-based chemical hydrides such as $LiNH_2$-LiH [5] and $NaBH_4$ [6,7] are expected as potential hydrogen sources for PEM fuel cells because of their high hydrogen contents [8]. Ammonia borane, NH_3BH_3, which has a hydrogen capacity of 19.6 wt.%, has made itself an attractive candidate for chemical hydrogen storage applications. Intensive efforts have been made to enhance the kinetics of hydrogen release from this compound from both solid and solution approaches [9–20].

A high performance hydrogen generation system based on transition metal-catalyzed dissociation and hydrolysis of NH_3BH_3 at room temperature has been achieved [12–20]. NH_3BH_3 dissolves in water to form a solution stable in the absence of air. The addition of a catalytic amount of suitable

* *Corresponding author*. Tel.: +81 72 751 9562; fax: +81 72 751 7942.
E-mail address: q.xu@aist.go.jp (Q. Xu).
0360-3199/$ – see front matter © 2009 International Association for Hydrogen Energy. Published by Elsevier Ltd. All rights reserved.
doi:10.1016/j.ijhydene.2009.03.003

metal catalysts into the solutions leads to rapid release of hydrogen gas with an H_2 to NH_3BH_3 ratio up to 3.0. Not only noble metals such as Pt, Ru, and Rh [12,15] but also non-noble metal-based catalysts such as Co, Ni, and Fe [14,16] exhibit high activities to this reaction. This hydrogen generation system possesses high potential to find its application in portable fuel cells. For practical use, low-cost and high performance non-noble metal catalysts are desired. Studies of catalysts for hydrogen generation from aqueous NH_3BH_3 solution show that dispersion of active metals and/or amorphousness of the active phase play important roles in catalytic performances [14–16,19,20]. However, few publications have reported the effect of dispersion and/or amorphousness of the active phase in nickel catalysts on the catalytic performance, and the cycle ability of the catalysts.

Colloidal metal dispersion can be easily obtained through dispersal in liquid media using water-soluble polymers, such as poly(N-vinyl-2-pyrrolidone) (PVP) [21–31]. PVP has received special attention because of its high chemical stability, non-toxicity, and excellent solubility in many polar solvents. PVP stabilized metals not only exhibit a high degree of metal dispersion but are also stabilized against agglomeration [23,26]. In addition, the polymer stabilized metals could be easily cross-linked by other polymers, and the cross-linked polymer stabilized metals have practical advantages for applications requiring recycling or fixed-bed operation, for example, easy separation and removal from the reactors [32–34].

The present paper reports that PVP stabilized nickel catalysts exhibit high durable performance for hydrogen generation from the hydrolysis of NH_3BH_3.

2. Experimental

2.1. *Experimental procedures for synthesis of nickel catalysts and hydrolysis of ammonia borane*

A mixture of sodium borohydride ($NaBH_4$, 20 mg, Aldrich, >98.5%) and ammonia borane (NH_3BH_3, 55 mg, Aldrich, 90%) was kept in a two-necked round-bottom flask. One neck was connected to a gas burette, and the other was fitted with a septum inlet to introduce 10 mL of aqueous nickel chloride hexahydrate ($NiCl_2 \cdot 6H_2O$, 38.12 mg, Kishida Chem. Co., >98%) solution mixed with poly(N-vinyl-2-pyrrolidone) (PVP, K-30, MW 40,000, 0, 0.1, 1, 10 mg, 0–0.045 mmol of monomeric units, respectively, Tokyo Kasei Chem. Ind. Co. Ltd.). The reaction started when the solution was syringed to the mixture of $NaBH_4$ and NH_3BH_3, and the evolution of gas was monitored using the gas burette. The reactions were carried out at 298 K in air.

After the hydrogen generation reaction was completed, new aqueous NH_3BH_3 solution (0.16 M, 10 mL) was added into the reaction flask. The evolution of gas was monitored using the gas burette. Such cycle tests of the catalyst for the hydrolysis of NH_3BH_3 were carried out five times in air.

All the samples after reaction were subjected to ultrafiltration (Ultrafilter Q0100, Advantec Co. Ltd.) under a pressure of nitrogen.

2.2. *Characterization*

The morphologies of the bare nickel catalyst and the PVP stabilized catalyst were observed using a Tecnai G^2 20 twin transmission electron microscope (TEM) operating with an acceleration voltage of 200 kV, which was equipped with a CCD camera (Gatan image filter) and an energy dispersive X-ray detector (EDX). Selected area electron diffraction (SAED) was obtained using a Hitachi H-9000NA transmission electron microscope (TEM) operating with an acceleration voltage of 300 kV. Samples for the measurements were prepared by placing a drop of a colloidal dispersion of the residue of filtration under a pressure of nitrogen in distilled water onto a copper grid, followed by drying in vacuum condition.

3. Results and discussion

Fig. 1 shows time courses of the hydrogen evolution from aqueous solutions of $NaBH_4$ and NH_3BH_3 mixtures catalyzed by Ni catalysts in air. The evolutions of 148 and 143 mL of hydrogen were finished in 12 and 9 min in the presence of $NiCl_2$ (Fig. 1a) and in the presence of $NiCl_2$ with PVP (Fig. 1b), respectively. As shown in the inset of Fig. 1b, only a negligible amount of hydrogen is evolved from the aqueous NH_3BH_3 solution without $NaBH_4$ in the presence of $NiCl_2$ with PVP. The result suggests that $NaBH_4$ is necessary for activating the catalyst, and Ni^{2+} is reduced via reaction (1).

$$Ni^{2+} + BH_4^- + 2H_2O \rightarrow Ni + BO_2^- + 2H^+ + 3H_2 \quad (1)$$

The effect of $NaBH_4$ has been reported for the Fe-catalyzed hydrolysis of NH_3BH_3 [13]. In the present reaction system, $NaBH_4$ was mixed with H_2O, NH_3BH_3, and the catalyst. Hydrogen is evolved via the following two reactions besides reaction (1):

$$NaBH_4 + 2H_2O \rightarrow Na^+ + BO_2^- + 4H_2 \quad (2)$$

$$NH_3BH_3 + 2H_2O \rightarrow NH_4^+ + BO_2^- + 3H_2 \quad (3)$$

Under the present reaction condition, about 40 mL of hydrogen is generated via reactions (1) and (2), and about 120 mL of hydrogen is generated via reaction (3), experimentally. The molar ratios of the hydrolytically generated hydrogen to the initial NH_3BH_3 both in the presence of the bare Ni catalyst and in the presence of the PVP stabilized Ni catalyst are 2.8 and 2.7, respectively. As the theoretical molar ratio at reaction completion is 3.0, the results indicate that the hydrolysis of NH_3BH_3 is almost completed in the presence of the bare Ni catalyst and in the presence of the PVP stabilized Ni catalyst.

The morphologies of the bare Ni catalyst and the PVP stabilized Ni catalyst after the hydrolysis of the $NaBH_4$ and NH_3BH_3 mixtures were examined by TEM measurements. The TEM and HAADF (high angle annular dark field) images of the bare Ni catalyst reveal that the catalyst contains grains with an amorphous structure

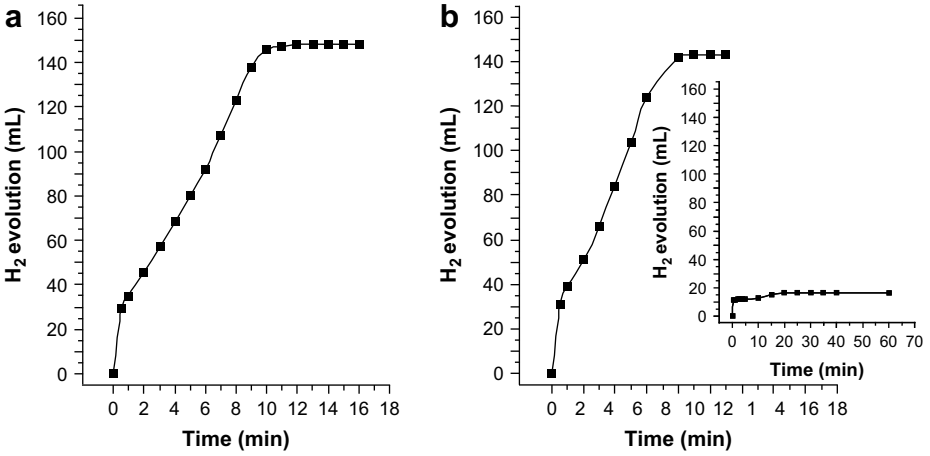

Fig. 1 – Hydrogen generation (a) in the presence of the bare Ni catalyst and (b) in the presence of the PVP stabilized Ni catalyst (PVP = 10 mg) from an aqueous solution of $NaBH_4$ and NH_3BH_3 (0.16 M, 10 mL) mixture and from an aqueous solution of NH_3BH_3 without $NaBH_4$ (inset of (b)). $Ni/NH_3BH_3 = 0.10$ at 298 K in air.

(Fig. 2a and b). Its related SAED pattern shown in Fig. 2c demonstrates the diffuse diffraction rings of an amorphous phase. Similar to the bare Ni catalyst, the TEM and HAADF images of the PVP stabilized Ni catalyst reveal that the catalyst also contains grains with an amorphous structure (Fig. 3a and b), and its SAED pattern shown in Fig. 3c demonstrates the diffuse diffraction rings of an amorphous phase.

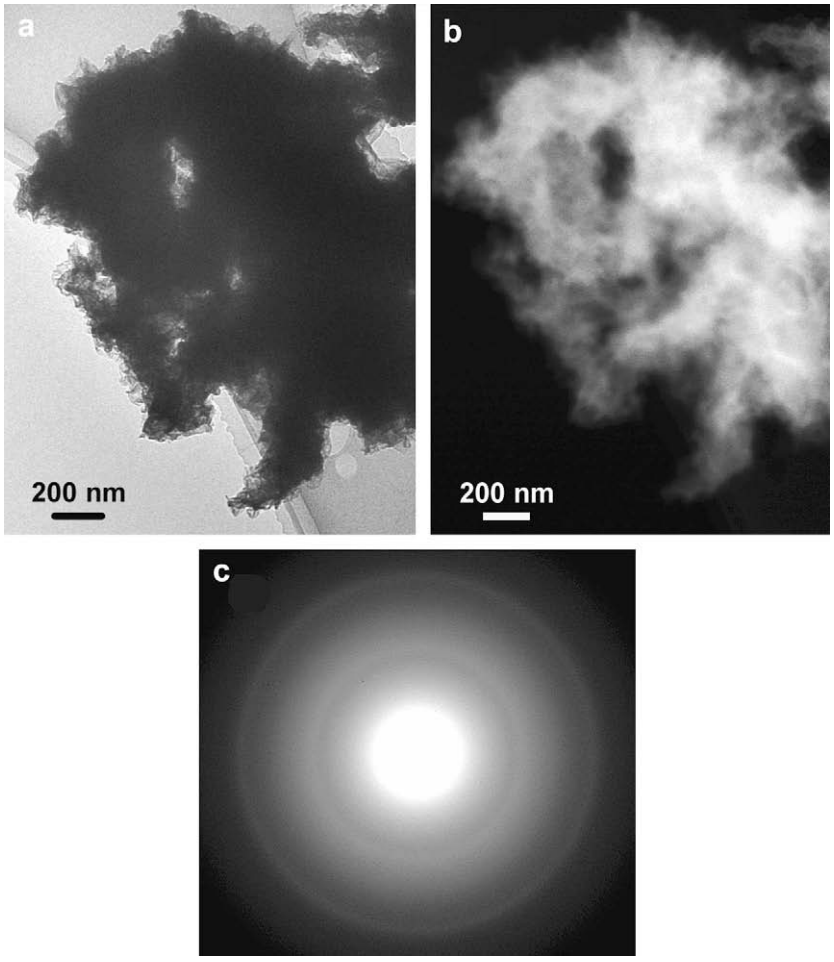

Fig. 2 – TEM (a) and HAADF (b) images of the bare Ni catalysts after hydrolysis of the solution of $NaBH_4$ and NH_3BH_3 mixture, and the corresponding SAED pattern (c).

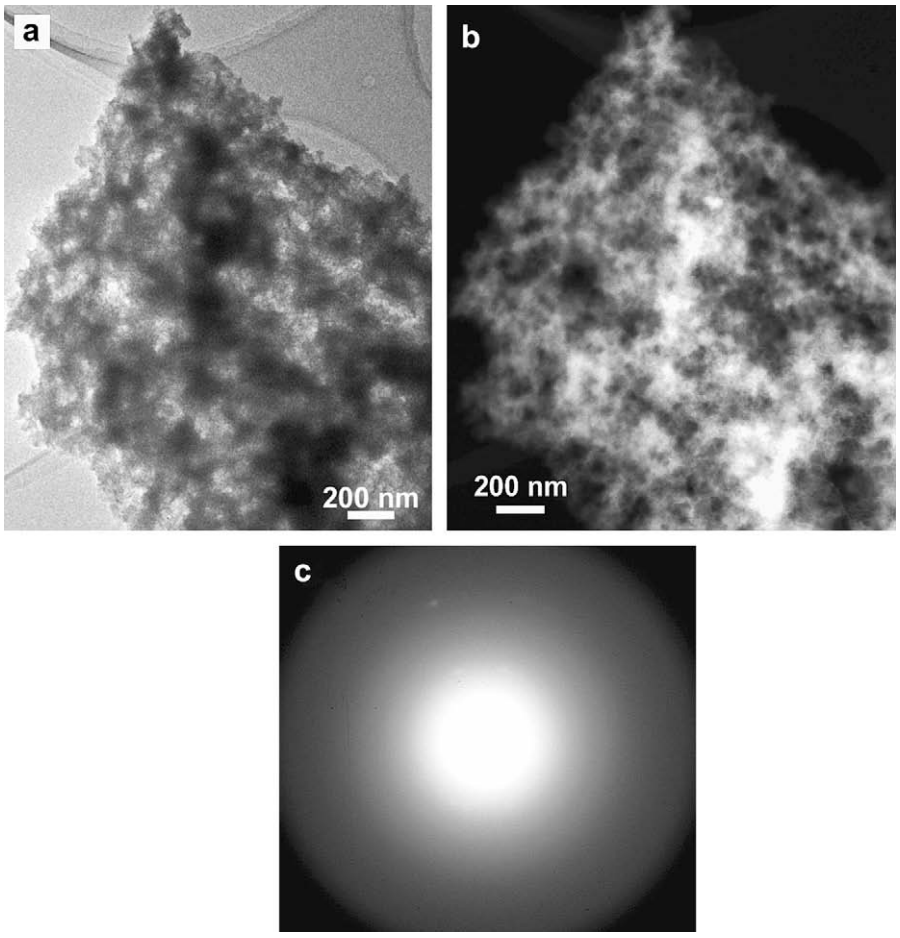

Fig. 3 – TEM (a) and HAADF (b) images of the PVP stabilized Ni catalysts (PVP = 10 mg) after hydrolysis of the $NaBH_4$ and NH_3BH_3 mixture, and the corresponding SAED pattern (c).

Fig. 4 shows time courses of the hydrogen evolution from aqueous NH_3BH_3 solutions catalyzed by Ni catalysts with various amounts of PVP (PVP = 0–10 mg) at the 1st and 5th cycle in air, respectively. The amount of hydrogen evolution does not depend on the amount of PVP, while the evolution rate significantly depends on the amount of PVP. At the 1st cycle, a stoichiometric amount of hydrogen was evolved in 33, 24, 24, and 14 min in the presence of the bare Ni catalyst and in the presence of the PVP stabilized Ni catalysts with PVP = 0.1, 1, and 10 mg, respectively. The results indicate that the PVP

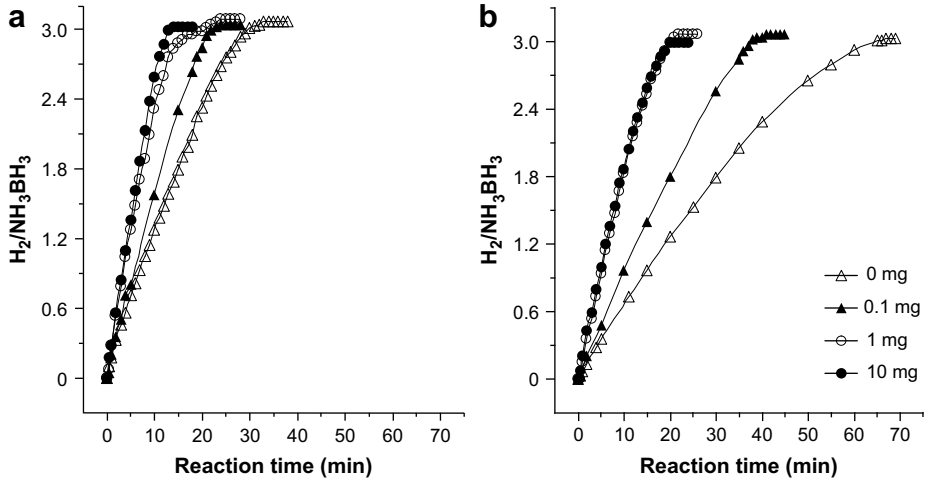

Fig. 4 – The H_2/NH_3BH_3 molar ratio of hydrogen generated from the aqueous solution (0.16 M, 10 mL) vs. reaction time catalyzed by the Ni catalyst with PVP = 0, 0.1, 1, and 10 at (a) the 1st cycle and (b) the 5th cycle (Ni/NH_3BH_3 = 0.10) at 298 K in air.

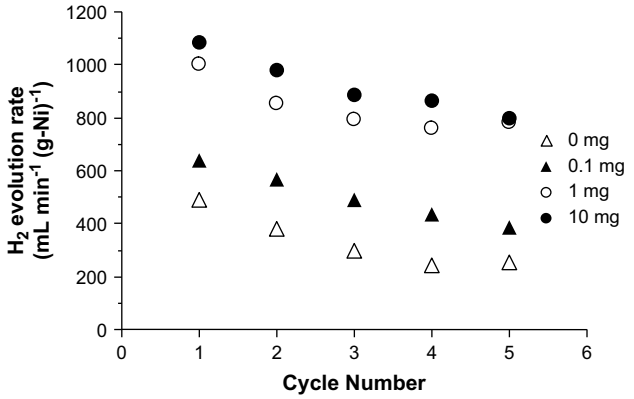

Fig. 5 – Hydrogen evolution rates for the uninterrupted cycle of Ni catalyst with PVP = 0, 0.1, 1, and 10 mg vs. the cycle number. Ni/NH_3BH_3 = 0.10 at 298 K in air.

stabilized Ni catalysts show higher hydrogen evolution rates than the bare Ni catalyst. At the 5th cycle, hydrogen evolution was finished in 67, 42, 22 and 20 min in the presence of the bare Ni catalyst and in the presence of the PVP stabilized Ni catalysts with PVP = 0.1, 1 and 10 mg, respectively. The results in Fig. 4a and b indicate that the hydrogen evolution rates are maintained in the presence of the PVP stabilized Ni catalysts with 1 and 10 mg, while the hydrogen evolution rates decrease in the presence of the bare Ni catalyst and in the presence of the PVP stabilized Ni catalysts with 0.1 mg. Fig. 5 shows the hydrogen evolution rates for the uninterrupted cycle of Ni catalysts. The evolution rates were calculated by averaging the hydrogen amounts evolved every minute in the range 5–50% of the maximum amounts evolved in the presence of each catalyst. At the 1st cycle, the PVP stabilized Ni catalysts with PVP = 1 and 10 mg show higher hydrogen evolution rates than the bare Ni catalyst and the PVP stabilized Ni catalyst with PVP = 0.1 mg. The evolution rates in the presence of the PVP stabilized Ni catalyst with PVP = 1 and 10 mg are 2.0 and 2.2 times, respectively, higher than that in the presence of the bare Ni catalyst. It is found that 78 and 74% of the evolution rates at the 1st cycle are retained at the 5th cycle in the presence of the PVP stabilized Ni catalysts with 1 and 10 mg, while 52 and 60% of the evolution rates at the 1st cycle are retained at the 5th cycle in the presence of the bare Ni catalyst and in the presence of the PVP stabilized Ni catalyst with PVP = 0.1 mg. The results indicate that PVP is an effective stabilizer to improve the durability of the Ni catalyst. Both the evolution rates in the presence of the PVP stabilized Ni catalysts with PVP = 1 and 10 mg are 3.1 times higher than that in the presence of the bare Ni catalyst.

The morphologies of the bare Ni catalyst and the PVP stabilized Ni catalyst after five cycles were examined by TEM

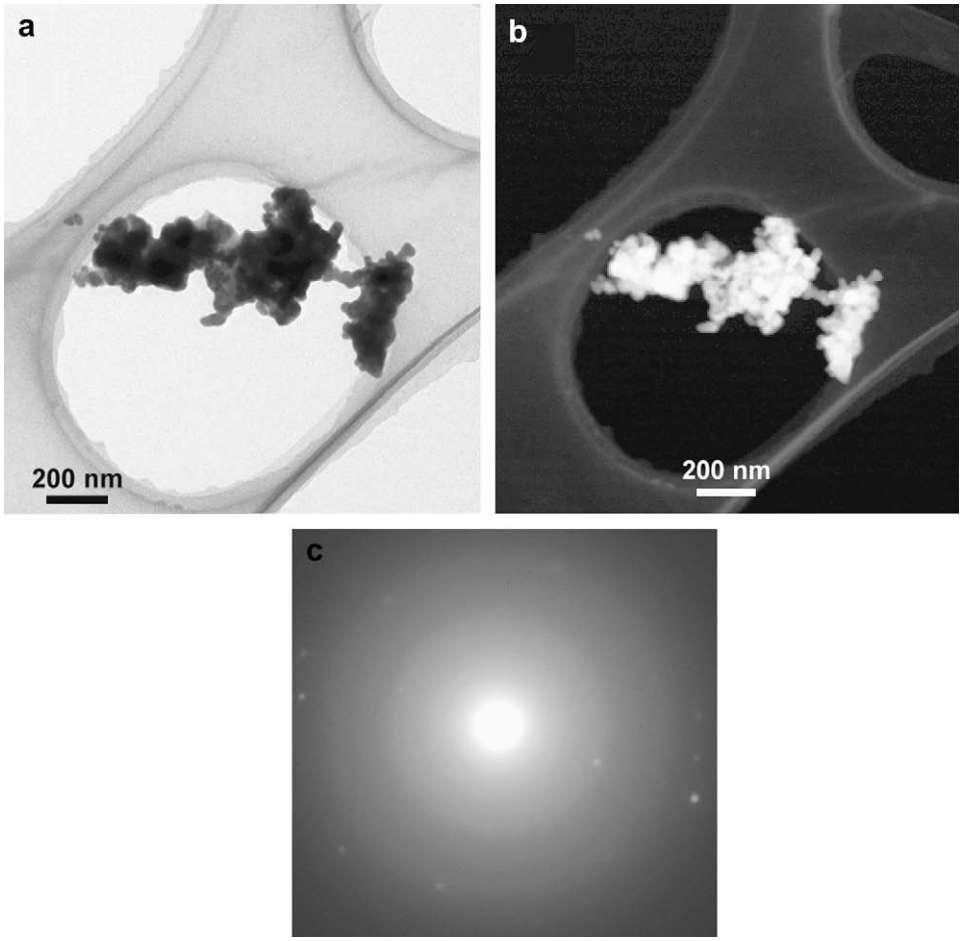

Fig. 6 – TEM (a) and HAADF (b) images of the bare Ni catalysts after five cycles, and the corresponding SAED pattern (c).

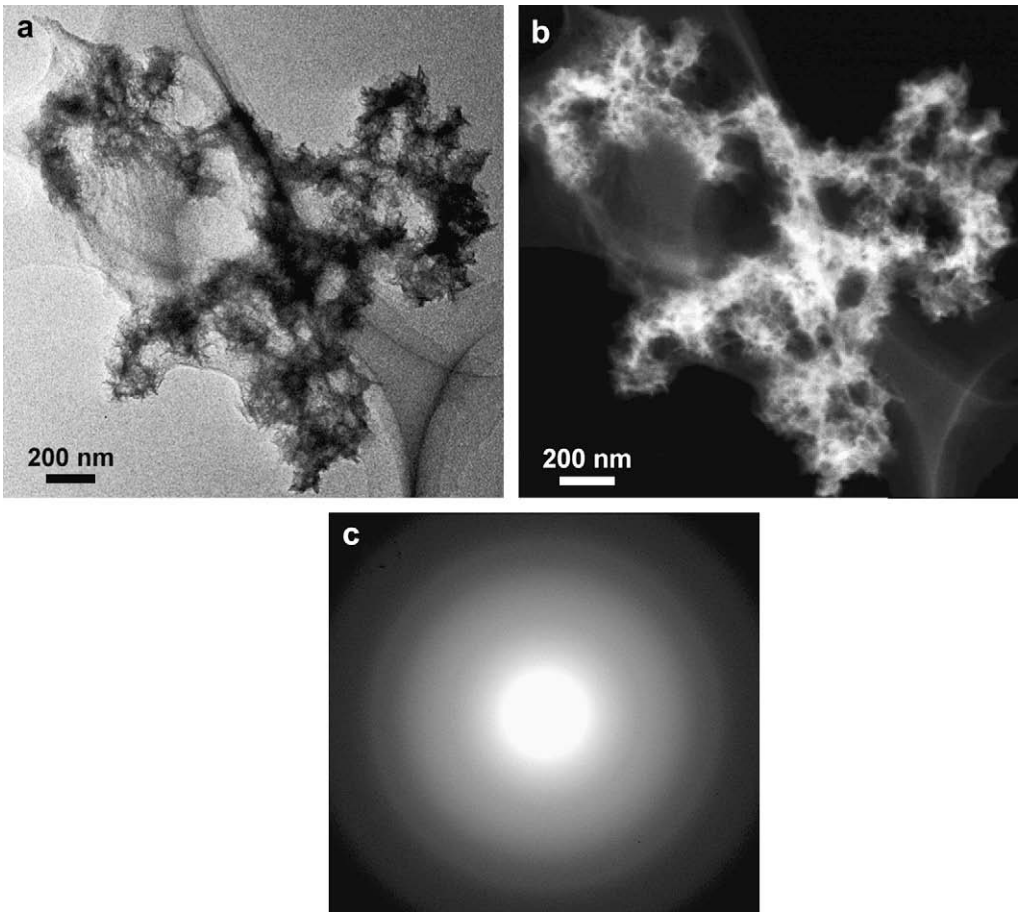

Fig. 7 – TEM (a) and HAADF (b) images of the PVP stabilized Ni catalysts (PVP = 10 mg) after five cycles, and the corresponding SAED pattern (c).

measurements. The TEM and HAADF images of the bare Ni catalyst reveal that the catalyst contains aggregates (Fig. 6a and b). The related SAED pattern shown in Fig. 6c demonstrates that the sample is polycrystalline. These results indicate that amorphous nickel in the bare Ni catalyst agglomerates and crystallizes during the reaction. The TEM and HAADF images of the PVP stabilized Ni catalyst reveal that the catalyst contains grains with an amorphous structure (Fig. 7a and b). The SAED pattern shown in Fig. 7c demonstrates diffuse diffraction rings of an amorphous phase. As shown in Fig. 3c, the PVP stabilized Ni catalyst also contains an amorphous structure after the hydrolysis of the $NaBH_4$ and NH_3BH_3 mixture. The results indicate that agglomeration and crystallization of nickel during the reaction can be prevented by the existence of PVP.

4. Conclusion

An amorphous nickel catalyst stabilized by poly(N-vinyl-2-pyrrolidone) was synthesized by reduction in an aqueous solution of $NaBH_4$ and NH_3BH_3 mixture, and amorphous nickel is identified both in the bare nickel catalyst and in the PVP stabilized nickel catalyst by TEM and HAADF measurements. The PVP stabilized nickel catalyst exhibits almost the same activity for the hydrolysis of NH_3BH_3 to generate almost a stoichiometric amount of hydrogen as the bare nickel catalyst. However, the PVP stabilized nickel catalyst shows higher durability than the bare nickel catalyst. Agglomeration and crystallization of amorphous nickel are observed for the bare nickel catalyst, whereas the PVP stabilized nickel catalyst maintains an amorphous structure after five cycles. The results indicate that PVP prevents agglomeration and crystallization of amorphous nickel, resulting in high durability.

Acknowledgement

The authors would like to thank NEDO and AIST for financial support and Mr. T. Uchida for TEM measurements.

REFERENCES

[1] Sperling D, DeLuchi MA. Transportation energy futures. Annu Rev Energy 1989;14:375–424.
[2] Schlapbach L, Züttel A. Hydrogen-storage materials for mobile applications. Nature 2001;414:353–8.

[3] Rosi NL, Eckert J, Eddaoudi M, Vodak DT, Kim J, O'Keeffe M, et al. Hydrogen storage in microporous metal-organic frameworks. Science 2003;300:1127–9.
[4] Deluga GA, Salge JR, Schmidt LD, Verykios XE. Renewable hydrogen from ethanol by autothermal reforming. Science 2004;303:993–7.
[5] Chen P, Xiong Z, Luo J, Lin J, Tan KL. Interaction of hydrogen with metal nitrides and imides. Nature 2002;420:302–4.
[6] Amendola SC, Sharp-Goldman SL, Saleem Janjua M, Kelly MT, Petillo PJ, Binder M. An ultrasafe hydrogen generator: aqueous, alkaline borohydride solutions and Ru catalyst. J Power Sources 2000;85(2):186–9.
[7] Amendola SC, Sharp-Goldman SL, Saleem Janjua M, Spencer NC, Kelly MT, Petillo PJ, et al. A safe, portable, hydrogen gas generator using aqueous borohydride solution and Ru catalyst. Int J Hydrogen Energy 2000;25(10):969–75.
[8] Umegaki T, Yan JM, Zhang XB, Shioyama H, Kuriyama N, Xu Q. Boron- and nitrogen-based chemical hydrogen storage materials. Int J Hydrogen Energy 2009;34(5):2303–11.
[9] Gutowska A, Li L, Shin Y, Wang CM, Li XS, Linehan JC, et al. Nanoscaffold mediates hydrogen release and the reactivity of ammonia borane. Angew Chem Int Ed Engl 2005;44(23):3578–82.
[10] Denney MC, Pons V, Hebden TJ, Heinekey DM, Goldberg KI. Efficient catalysis of ammonia borane dehydrogenation. J Am Chem Soc 2006;128(37):12048–9.
[11] Keaton RJ, Blacquiere JM, Baker RT. Base metal catalyzed dehydrogenation of ammonia-borane for chemical hydrogen storage. J Am Chem Soc 2007;129(7):1844–5.
[12] Chandra M, Xu Q. A high-performance hydrogen generation system: transition metal-catalyzed dissociation and hydrolysis of ammonia-borane. J Power Sources 2006;156(2):190–4.
[13] Chandra M, Xu Q. Dissociation and hydrolysis of ammonia-borane with solid acids and carbon dioxide: an efficient hydrogen generation system. J Power Sources 2006;159(2): 855–60.
[14] Xu Q, Chandra M. Catalytic activities of non-noble metals for hydrogen generation from aqueous ammonia-borane at room temperature. J Power Sources 2006;163(1):364–70.
[15] Chandra M, Xu Q. Room temperature hydrogen generation from aqueous ammonia-borane using noble metal nano-clusters as highly active catalysts. J Power Sources 2007;168(1):135–42.
[16] Yan JM, Zhang XB, Han S, Shioyama H, Xu Q. Iron-nanoparticle-catalyzed hydrolytic dehydrogenation of ammonia borane for chemical hydrogen storage. Angew Chem Int Ed Engl 2008;47(12):2287–9.
[17] Cheng F, Ma H, Li Y, Chen J. $Ni_{1-x}Pt_x$ ($x = 0$–0.12) hollow spheres as catalysts for hydrogen generation from ammonia borane. Inorg Chem 2007;46(3):788–94.
[18] Yao CF, Zhuang L, Cao YL, Ai XP, Yang HX. Hydrogen release from hydrolysis of borazane on Pt- and Ni-based alloy catalysts. Int J Hydrogen Energy 2008;33(10):2462–7.
[19] Kalidindi SB, Indirani M, Jagirdar BR. First row transition metal ion-assisted ammonia-borane hydrolysis for hydrogen generation. Inorg Chem 2008;47(16):7424–9.
[20] Kalidindi SB, Sanyal U, Jagirdar BR. Nanostructured Cu and $Cu@Cu_2O$ core shell catalysts for hydrogen generation from ammonia-borane. Phys Chem Chem Phys 2008;10(38):5870–4.
[21] Toshima N, Wang Y. Preparation and catalysis of novel colloidal dispersions of copper/noble metal bimetallic clusters. Langmuir 1994;10(12):4574–80.
[22] Wang Y, Liu H, Toshima N. Nanoscopic naked Cu/Pd powder as air-resistant active catalyst for selective hydration of acrylonitrile to acrylamide. J Phys Chem 1996;100(50):19533–7.
[23] Bonet F, Delmas V, Grugeon S, Herrera Urbina R, Silvert PY, Tekaia-Elhsissen K. Synthesis of monodisperse Au, Pt, Pd, Ru, and Ir nanoparticles in ethylene glycol. Nanostruct Mater 1999;11(8):1277–84.
[24] Chou KS, Huang KC. Studies on the chemical synthesis of nanosized nickel powder and its stability. J Nanopart Res 2001;3(2–3):127–32.
[25] Pastoriza-Santos I, Liz-Marzán LM. Synthesis of silver nanoprisms in DMF. Nano Lett 2002;2(8):903–5.
[26] Narayanan R, El-Sayed MA. Effect of catalysis on the stability of metallic nanoparticles: Suzuki reaction catalyzed by PVP-palladium nanoparticles. J Am Chem Soc 2003; 125(27):8340–7.
[27] Tsunoyama H, Sakurai H, Ichikuni N, Negishi Y, Tsukuda T. Colloidal gold nanoparticles as catalyst for carbon–carbon bond formation: application to aerobic homocoupling of phenylboronic acid in water. Langmuir 2004;20(26):11293–6.
[28] Liaw BJ, Chiang SJ, Tsai CH, Chen YZ. Preparation and catalysis of polymer-stabilized NiB catalysts on hydrogenation of carbonyl and olefinic groups. Appl Catal A: Gen 2005;284(1–2):239–46.
[29] Washio I, Xiong Y, Yin Y, Xia Y. Reduction by the end groups of poly(vinyl pyrrolidone): a new and versatile route to the kinetically controlled synthesis of Ag triangular nanoplates. Adv Mater 2006;18(13):1745–9.
[30] Shengming J, Liangsheng Y, Ying Z, Guanzhou Q, Cuifeng W. Study on thermodynamics and oxidation mechanism of ethylene glycol in the preparation of nanometer nickel powders. Mater Res Bull 2006;41(11):2130–6.
[31] Zhang J, Lan CQ. Nickel and cobalt nanoparticles produced by laser ablation of solids in organic solution. Mater Lett 2008;62(10–11):1521–4.
[32] Nádasdi L, Joó F, Horváth I, Vígh L. Colloidal metal dispersions as catalysts for selective surface hydrogenation of biomembranes. Part 2. Preparation of nanosize platinum metal catalysts and characterization in hydrogenation of water soluble olefins and synthetic biomembrane models. Appl Catal A: Gen 1997;162(1–2):57–69.
[33] De Blasio N, Tempesti E, Kaddouri A, Mazzocchia C, Cole-Hamilton DJ. Activity and stability of two polymer-supported rhodium-based catalysts for the vapour phase carbonylation of methanol. J Catal 1998;176(1):253–9.
[34] Hafez HS, El-Hag Ali A, Abdel-Mottaleb MSA. Photocatalytic efficiency of titanium dioxide immobilized on PVP/AAc hydrogel membranes: a comparative study for safe disposal of wastewater of Remazol Red RB-133 textile dye. Int J Photoenergy 2005;7(4):181–5.